Oil & Gas Science and Technology - Rev. IFP Energies nouvelles (2017) **72**, 35

DOI: 10.2516/ogst/2017030

Experimental Study and Performance Investigation of Miscible Water-Alternating-CO_2 Flooding for Enhancing Oil Recovery in the Sarvak Formation

Vahid Rahimi[1,*], Mohammad Bidarigh[1] and Peyman Bahrami[2]

[1] Department of Petroleum Engineering, Science and Research Branch, Islamic Azad University, Tehran - Iran
[2] Young Researchers and Elites Club, Science and Research Branch, Islamic Azad University, Tehran - Iran
e-mail: vahid_rahimi2010@yahoo.com

*Corresponding author

Abstract *— This experimental study is aimed at evaluating the performance of the miscible Water-Alternating-CO_2 (CO_2-WAG) flooding as a function of slug size and WAG ratio based on the ultimate oil recovery in the Sarvak formation. In this research, initially the slim-tube apparatus was used to determine the Minimum Miscibility Pressure (MMP) of the Sarvak heavy oil and CO_2 at the constant reservoir temperature. Then, a total of seven core flooding experiments were performed by using the sandstone core samples collected from the Sarvak formation. These experiments were conducted through respective water flooding, miscible continuous CO_2 flooding, and miscible CO_2-WAG flooding. In the miscible CO_2-WAG flooding, different WAG slug sizes of 0.15, 0.25, and 0.50 Pore Volume (PV) and different WAG ratios of 1:1, 2:1, and 1:2 were applied to investigate their effects on the oil Recovery Factor (RF) in the Sarvak formation. The results showed that, in general, the miscible CO_2 Enhanced Oil Recovery (CO_2-EOR) process is capable of mobilizing the heavy oil and achieving a high and significant oil RF in the Sarvak formation. The miscible CO_2-WAG flooding has the highest oil RF (84.3%) in comparison with water flooding (37.7%), and miscible continuous CO_2 flooding (61.5%). In addition, using a smaller WAG slug size for miscible CO_2-WAG flooding leads to a higher oil RF. The optimum WAG ratio of the miscible CO_2-WAG flooding for the Sarvak formation is approximately 2:1. The results also demonstrated that, more than 50% of the heavy oil is produced in the first two cycles of the miscible CO_2-WAG flooding. The optimum miscible CO_2-WAG flooding has a much less CO_2 consumption than the miscible continuous CO_2 flooding.*

INTRODUCTION

In recent decades, the high price of oil and the growing demands of oil have led to the development of various Enhanced Oil Recovery (EOR) methods. CO_2 is used extensively in EOR techniques due to its low injectivity problems, low formation volume factor, low Minimum Miscibility Pressure (MMP), abundance of reserves, and high incremental oil recovery compared to other gases (Majidaie *et al.*, 2013). Theoretical investigations on the application of CO_2 for EOR started in the early 20th century (Rogers and Grigg, 2000). Over the past few decades, extensive laboratory studies, numerical simulations, and field applications of CO_2-EOR processes have been reported (Burke *et al.*, 1990; Grigg and Schecter, 1993; Idem and Ibrahim, 2002; Moritis, 2006; Chukwudeme and Hamouda, 2009; Hamouda *et al.*, 2009; Manrique *et al.*, 2010; Enick and Olsen, 2012). Several CO_2-EOR methods have been suggested and developed, such as continuous CO_2 flooding and Water-

Alternating-CO_2 (CO_2-WAG) flooding under immiscible and miscible displacements. Continuous CO_2 flooding is considered as one of the largest utilized EOR methods which is proven as a highly effective EOR method in the petroleum industry (Alquriaishi and Shokir, 2011). The main displacement mechanisms for improved oil recovery during the CO_2-EOR include CO_2-oil Interfacial Tension (IFT) reduction, oil swelling, oil viscosity reduction, solution gas drive, and extraction of light and intermediate hydrocarbons for immiscible CO_2 flooding to completely miscible displacement (Blunt *et al.*, 1993; Tunio *et al.*, 2011; Cao and Gu, 2013; Song *et al.*, 2014). In miscible displacement, CO_2 is fully mixed with the reservoir oil causing oil swelling and viscosity reduction. This reduction of the viscosity in heavy oil is higher compared to light oil (Baviere, 1991; Agbalaka *et al.*, 2008; Sohrabi *et al.*, 2008). Despite these advantages, continuous CO_2 flooding has some limitations both technically and economically. Technically, since CO_2 is injected under supercritical conditions, its viscosity is less than most types of crude oils, which can lead to viscous fingering, gravity override, and the formation of preferential paths in the reservoir rock (Bednarz and Stopa, 2014). This problem causes an early CO_2 Breakthrough (BT) and a reduction of volumetric sweep efficiency. Economically, a large amount of CO_2 is needed in continuous CO_2 flooding. Relatively high operating costs of CO_2 transportation, storage, and compression may seriously limit many field applications of continuous CO_2 flooding (Holt *et al.*, 2009).

To improve the volumetric sweep efficiency and reduce the amount of CO_2 needed for continuous CO_2 flooding, CO_2 is typically injected into the reservoir alternately with water. This process is called CO_2-WAG flooding. The first field application of WAG flooding was done in the North Pembina oil field in Alberta, Canada, by *Mobil* in 1957 (Christensen *et al.*, 2001; Mirkalaei *et al.*, 2011). The CO_2-WAG flooding is the combination of the improved volumetric sweep efficiency of water flooding with the enhanced microscopic displacement efficiency of CO_2 flooding, which can lead to a better displacement and an increase of oil recovery compared to continuous CO_2 flooding or water flooding (Christensen *et al.*, 1998, 2001; Sohrabi *et al.*, 2004; Kulkarni and Rao, 2005; Dehghan *et al.*, 2009; Rouzbeh and Larry, 2010). On the other hand, in the CO_2-WAG flooding, the injected CO_2 reduces the oil viscosity while water sweeps the mobilized oil to the production well (Ghedan, 2009). Apart from the technical advantages mentioned, economically, the CO_2-WAG flooding can considerably reduce CO_2 consumption in comparison with continuous CO_2 flooding. In a review of 59 WAG flooding field applications by Christensen *et al.* (2001), which 24 of those projects were miscible CO_2-WAG flooding, it has been reported that most CO_2-WAG flooding projects result in an increase of average oil recovery of 5–10% Original Oil in Place (OOIP) (Christensen *et al.*, 2001; Skauge and Stensen, 2003).

The main factors influencing the WAG flooding include reservoir wettability, reservoir heterogeneity, reservoir rock and fluid properties, injection techniques, and WAG parameters (slug size and WAG ratio) (Righi and Pascual, 2007). Two of the most important economic parameters affecting the WAG flooding are slug size and WAG ratio. The slug size refers to the volume of the injected CO_2 in each WAG cycle. The slug volume is usually expressed as a percentage of rock Pore Volume (PV) (Farouq, 2003). The optimum CO_2 slug size is critical in a proper design of miscible WAG flooding (Gale, 2003). The optimum CO_2 slug size for a particular project depends on economical factors such as crude price, CO_2 cost, and the amount and timing of the incremental recovery. The ultimate CO_2 slug size can be determined after the start of project, when more information is known about future price of oil and production response of the reservoir. The WAG ratio is very important in CO_2-WAG flooding design (Chen *et al.*, 2010; Farshid *et al.*, 2010). An optimum WAG ratio has a significant effect on operations and economics of a CO_2 flooding. The WAG ratio is defined as the ratio of the injected water volume to CO_2 volume in each WAG cycle (Farouq, 2003). To maximize the net present value of CO_2 flooding, the WAG ratio should be increased gradually after achieving optimum CO_2 production (Christensen *et al.*, 1998). The gradual increase of the injected water results in increased mobility control and a constant produced CO_2 profile. If the WAG ratio is low, the injected excessive CO_2 will flow much faster than the injected water, which leads to an early CO_2 BT and a low volumetric sweep efficiency (Rao and Girard, 2002). Therefore, it is required to determine the optimum WAG ratio for WAG flooding process.

Although numerous experimental studies and numerical simulations have been performed in the past to investigate the CO_2-WAG flooding processes in various oil reservoirs, so far fewer studies have been done on the miscible CO_2-WAG flooding processes through the real reservoir core samples in heavy oil formations. The Sarvak formation has a heavy oil with *American Petroleum Institute* (API) gravity of 18.81° and approximately 30 billion barrels of the OOIP, which is located in south-western Iran. In this research, a number of sandstone core samples were taken from the Sarvak formation in Iran. Several slim-tube experiments were done at different displacement pressures and the constant reservoir temperature. Then, the MMP between the Sarvak heavy oil and CO_2 was determined by plotting the oil RF *versus* displacement pressure. A total of seven core flooding experiments were conducted to measure the oil RF and oil production of different CO_2-EOR methods. The following CO_2-EOR processes were examined and

TABLE 1
Physical properties and analysis of dead oil sample.

Specification	Unit	Quantity
Specific gravity @ 15.56/15.56 °C	–	0.9414
°API	–	18.81
Sulphur content	wt%	3.75
H_2S content	ppm	<1.0
Nitrogen total	wt%	0.17
Water content	vol%	2.0
Salt content	vol%	320.0
Viscosity @ 20 °C	c.p.	167.5
Viscosity @ 40 °C	c.p.	49.96
Viscosity @ 96.1 °C	c.p.	7.62
Pour point	°C	−18
Asphaltene content	wt%	12.8
Wax content	wt%	4.0
Carbon residue	wt%	12.18
Acidity total	mgKOH/g	0.95
Nickel	ppm	31.0
Vanadium	ppm	121.0
Iron	ppm	32.0
Lead	ppm	<1.0
Sodium	ppm	0.63

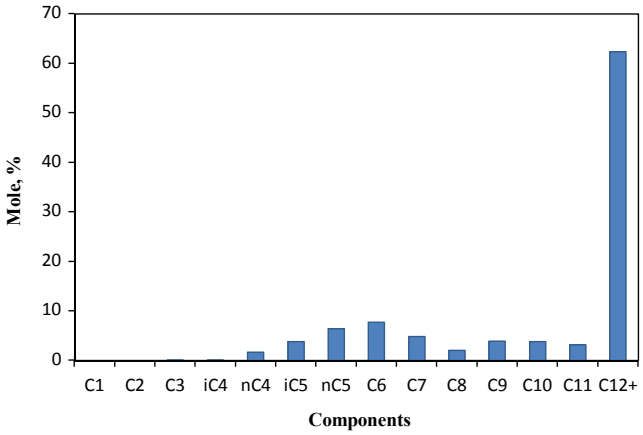

Figure 1
Compositional analysis results of dead oil sample.

TABLE 2
Compositional analysis results of reservoir brine.

Component	Unit	Quantity
Potassium	mg/L	920
Sodium	mg/L	108000
Calcium	mg/L	3600
Magnesium	mg/L	500
Strontium	mg/L	190
Iron	mg/L	19
Zinc	mg/L	7
Manganese	mg/L	1.6
Silicon	mg/L	4
Sulfate	mg/L	2370
Chloride	mg/L	174000
Bicarbonate	mg/L	300
TDS	mg/L	290000

compared: three different flooding methods of water flooding, miscible continuous CO_2 flooding, and miscible CO_2-WAG flooding; three different WAG slug sizes of 0.15, 0.25, and 0.50 PV; three different WAG ratios of 1:1, 2:1, and 1:2. In general, the main objective of this work is the performance evaluation of the miscible CO_2-WAG flooding process as a function of slug size and WAG ratio based on ultimate oil recovery in the Sarvak formation.

1 EXPERIMENTAL DETAILS

1.1 Materials

In this study, the oil sample and reservoir brine were collected from the Sarvak formation of Azadegan oilfield in Ahvaz, Iran. The oil sample is heavy gravity (18.81 API). The physical properties and detailed analysis of Stock Tank (dead) oil sample are listed in Table 1. Also, the compositional analysis of dead oil sample used in all experiments is shown in Figure 1. As can be seen, the total molar percentages of $C_{1\text{-}11}$ and C_{12+} are equal to 37.65 and 62.35 mol%, respectively. These data show that the oil sample contains a large amount of heavy components. The composition of reservoir brine, which PH at the ambient temperature is equal to 6.5, is given in Table 2. However, a synthetic brine was prepared for the core flooding experiments. The synthetic brine contained 290000 mg/L (ppm) NaCl, which was equal to the Total Dissolved Solids (TDS) of the reservoir brine.

CO_2 with a purity of 99.998 mol% was used in this study as the injecting gas. The density and viscosity of CO_2 at the reservoir pressure of 26.20 MPa and $T_{res} = 96.1$ °C were equal to 0.596 g/cc and 0.0487 cp, respectively. These data

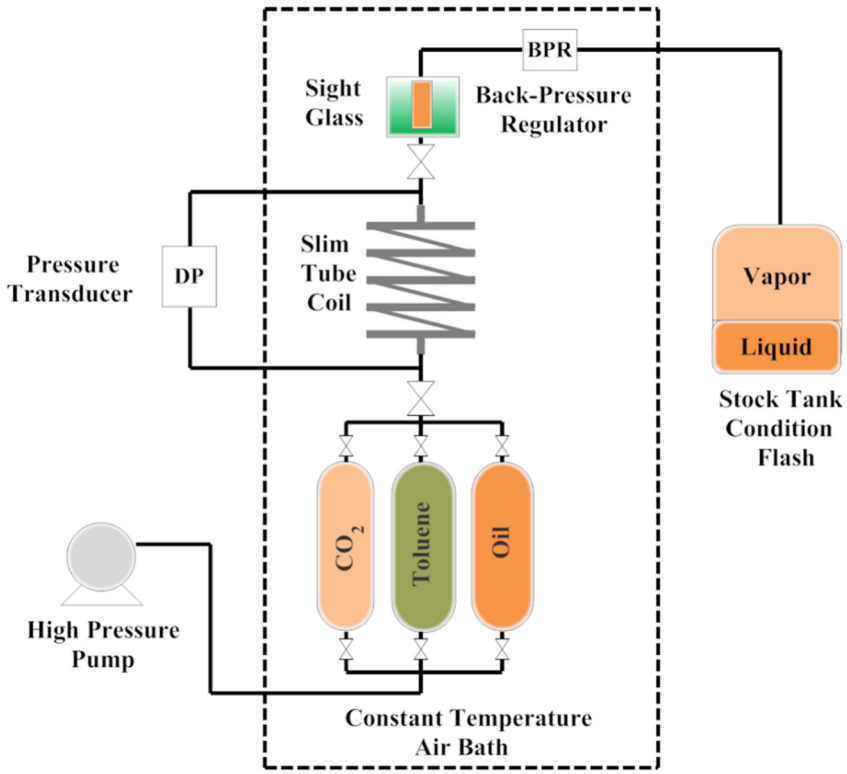

Figure 2

Schematic diagram of slim-tube apparatus.

were calculated by using the PVTi module of ECLIPSE Simulation Software with 3-Parameter Peng-Robinson equation of state.

A number of sandstone core samples were taken from the Sarvak formation of Azadegan oilfield in the same region where oil and brine samples were collected. The diameter of these samples was equal to 3.8 cm. Also, the length, porosity, and permeability of the collected core samples were in the range of 15.50–19.50 cm, 15.46–19.05%, and 23.40–46.61 md, respectively.

1.2 Miscibility (Slim-Tube) Apparatus

The first slim-tube experiment has been done in the early 1950s. The slim-tube apparatus is widely considered as a standard method in the industry for estimating MMP. Figure 2 shows a schematic diagram of the slim-tube apparatus. The slim-tube apparatus has three main sections: slim-tube coil; upstream and downstream sections.

The slim-tube coil (porous media) has a narrow and long stainless-steel coiled tubing with an inner diameter of 0.635 cm and a length of 1200 cm (to a one-dimensional displacement and minimize the viscous fingering and gravity segregation). The tube was packed with glass beads of 100 mesh size to create a porous media. The porosity and permeability of porous media were equal to 35% and 3000 md, respectively. The permeability of porous media is high and the pressure drop across the slim-tube coil was minimized. The slim-tube coil was placed in an air bath to maintain the reservoir temperature.

The upstream section consists of three piston accumulators (oil, CO_2, and toluene) and a high pressure pump. The CO_2 accumulator was placed inside the air bath to create the reservoir temperature conditions for CO_2. The accumulators were connected to the high pressure pump to move the fluids into the slim-tube coil.

The downstream section consists of a sight glass and a Back-Pressure Regulator (BPR). The sight glass was generally applied to visual inspection of the produced fluids and help in determination of miscibility conditions. The BPR was placed in the air bath and was used to maintain the pressure inside the slim-tube coil. Finally, in the outlet of slim-tube apparatus, the produced fluids were separated and collected after the BPR at the atmospheric pressure. It should be noted that the pressure drop across the slim-tube coil was measured using a pressure transducer.

1.3 Core Flooding Apparatus

The core flooding apparatus is designed to carry out the core flooding experiments at high pressure and temperature. A schematic diagram of the core flooding apparatus used in

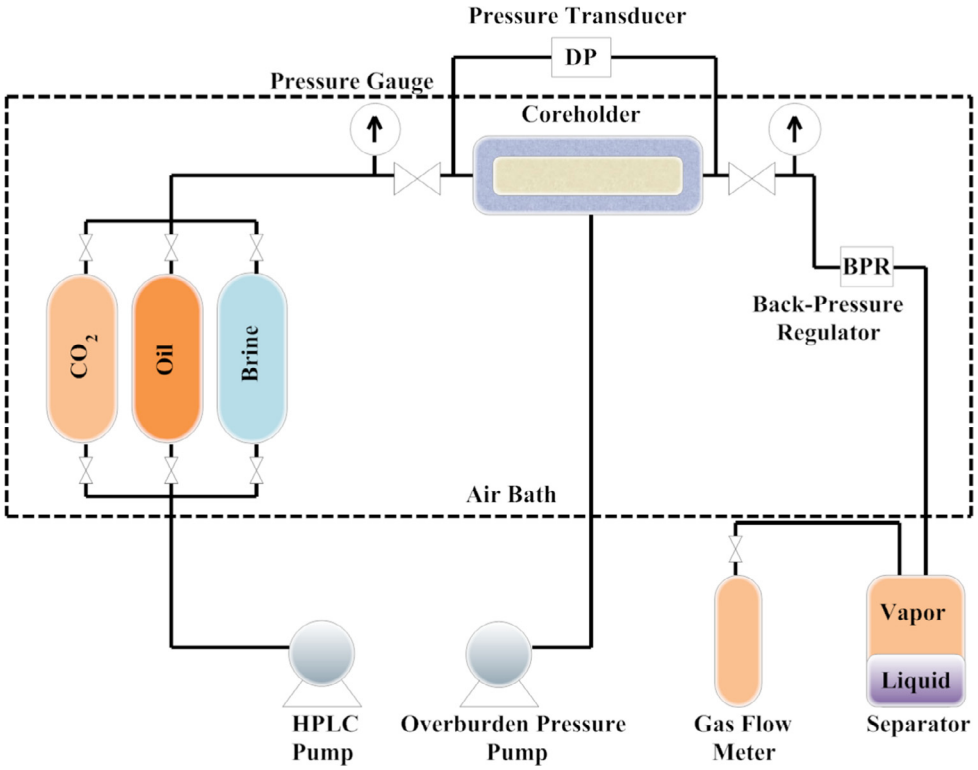

Figure 3

Schematic diagram of core flooding apparatus.

this study is shown in Figure 3. The apparatus consists of four main sub-systems: injection system; displacement system; production system; and temperature control system.

In the fluid injection system, a High Performance Liquid Chromatography (HPLC) pump was used to inject the fluids stored in transfer cylinders (oil, CO_2, and brine) into the core samples at a constant rate. The distilled water was transported from the HPLC pump to the bottom of floating piston transfer cylinders to move the piston upward and compact the desired fluids.

The fluids displacement under actual reservoir conditions occurred inside the core samples placed in the core holder. The high pressure nitrogen was pumped by using a high pressure syringe pump to supply overburden pressure to the core holder, which is usually between 3.0–5.0 MPa higher than the injection pressure. The pressure transducer was used to measure the pressure drop across the core samples.

In the production system, a BPR was used to produce a constant production pressure during the core flooding experiments. Finally, the produced fluids (oil, CO_2, and brine) were collected and separated in a separator. The CO_2 production was measured by using a gas flow meter.

The fluids transfer cylinders, core holder, BPR, and flow lines were placed inside an air bath. A heater and a temperature controller were used to heat the air bath and maintain the constant reservoir temperature of 96.1 °C.

2 EXPERIMENTAL PROCEDURE

In this section, the MMP determination procedure by slim-tube apparatus and the core flooding experiments are described in detail. In all experiments, the supercritical CO_2 and synthetic brine were injected to displace dead oil.

2.1 Slim-Tube Experiments

The slim-tube displacement experiments were run to determine the MMP needed to establish dynamic miscibility of the Sarvak heavy oil sample with CO_2 at the reservoir temperature. To do the slim-tube experiments, the porous media in the tube was first saturated with the Sarvak oil sample. The coiled tube was maintained at the reservoir temperature and a pressure above the bubble point pressure ($P_b = 9.87$ MPa) by using the air bath and BPR, respectively. Then, to displace oil, CO_2 was injected into the tube at a constant rate of 0.2 cc/min. Generally, the pressure drop across the coiled tube is very small, so, the entire displacement pressure is considered to be constant. The experiments were completed when 1.2 PV of CO_2 was injected. The slim-tube experiments were done at several different pressures at the reservoir temperature. In each experiment, the oil RF after 1.2 PV of CO_2 injected was recorded. By plotting the oil RF at each displacement

TABLE 3
Physical properties of core samples.

Experiment No.	Porosity (%)	Permeability (md)	Connate water saturation (%)	Initial oil saturation (%)
1	18.22	23.40	27	73
2	19.05	30.21	19	81
3	18.41	28.34	20	80
4	16.40	28.63	18	82
5	15.46	25.82	17	83
6	17.65	40.26	22	78
7	16.35	46.61	23	77

pressure *versus* pressure, the MMP value was obtained. The most common criterion for the MMP determination was used, namely the curve break-over point in this plot (Ahmadi, 2011). It should be noted that before and after each experiment run, the slim-tube coil was cleaned with toluene.

2.2 Core Flooding Experiments

Seven experiments were run on the 7 core samples taken from the Sarvak formation with various properties to investigate the performance of the miscible CO_2-WAG flooding process. These experiments were examined in the form of three scenarios. In the first scenario, the different flooding methods like water flooding, miscible continuous CO_2 flooding, and miscible CO_2-WAG flooding were compared to investigate the effect of each of them on the oil RF and select the optimum method. In the second and third scenarios, a series of miscible CO_2-WAG floodings were performed and the optimum slug size and WAG ratio were determined.

Before the core flooding experiments, the sandstone core samples were cleaned with toluene, methanol, and chloroform to remove hydrocarbons, salts, and clays, respectively and dried. After preparing the core samples, they were placed horizontally inside the core holder and evacuated by using a vacuum pump. Then, the core samples were saturated using the synthetic brine to measure the porosities. By weighing the dried and wetted core samples and using the density of the synthetic brine, the PV was calculated (Eq. 1). Therefore, by knowing the Bulk Volume (BV), the porosity of the core samples was determined using Equation (2).

$$\mathrm{PV} = (W_{\mathrm{wet}} - W_{\mathrm{dry}})/\rho_{\mathrm{brine}}. \quad (1)$$

$$\varphi = \mathrm{PV}/\mathrm{BV}. \quad (2)$$

After porosity determination, the absolute permeability of the core samples was measured by injecting the synthetic brine at different flow rates and the corresponding pressure drops measurement. At first, the synthetic brine was injected with a low flow rate to reach the steady state flow conditions. The Darcy's law was applied to calculate t absolute permeability which can be rearranged as follows:

$$q\mu/A = k\Delta p/L, \quad (3)$$

where q is the flow rate, μ is the viscosity of the synthetic brine, A is the cross-sectional area of the core samples, k is the absolute permeability of the core samples, ΔP is the pressure drop across the core samples, and L is the length of the core samples. By plotting $q\mu/A$ *versus* $\Delta P/L$ and using the linear regression, the absolute permeability of the core samples was calculated which is equivalent to the slope of the straight line fitted to the data.

After measuring the absolute permeability, the Sarvak heavy oil was injected into the core samples saturated with the synthetic brine at a constant rate of 0.2 cc/min in order to achieve the connate water saturation. By knowing the initial volume of the synthetic brine inside the core samples and the volume of the effluent brine, the connate water saturation was calculated. Also, the initial oil saturation was obtained by knowing the volume of the oil injected and the PV of the core samples. The measured porosity, absolute permeability, connate water saturation, and initial oil saturation of core samples used in this study have been shown in Table 3.

In order to carry out the flooding experiments at the reservoir conditions, after preparing the core samples and reaching the connate water saturation and the initial oil saturation, a heater and a temperature controller were used to increase the air bath temperature from ambient to 96.1 °C (reservoir temperature) and maintain this temperature.

In the water flooding experiment (experiment 1), after the core sample was pressurized to 26.20 MPa, the synthetic brine was injected at a constant injection rate of 0.2 cc/min and $T_{\mathrm{res}} = 96.1$ °C. The brine flooding was continued until no more oil was produced (1.5 PV of the synthetic brine was injected).

In the miscible continuous CO_2 flooding experiment (experiment 2), the supercritical CO_2 was injected at a constant injection rate of 0.2 cc/min and $T_{\mathrm{res}} = 96.1$ °C. The

production pressure was set to be 26.20 MPa which is higher than the MMP of CO_2. The CO_2 flooding was continued until no more oil was produced (2.25 PV of CO_2 was injected).

In the miscible CO_2-WAG flooding experiments (experiments 3–7), the supercritical CO_2 and synthetic brine were injected into the core samples alternately at the same constant injection rate of 0.2 cc/min, the production pressure of 26.20 MPa, and T_{res} = 96.1 °C with the different slug sizes of 0.15, 0.25, and 0.50 PV (experiments 3–5) and the different WAG ratios of 1:1, 2:1, and 1:2 (experiments 3, 6, and 7). The CO_2 and brine flooding alternately in each miscible CO_2-WAG flooding experiment was continued until no more oil was produced.

It should be noted that, in all of miscible CO_2-WAG flooding experiments, the first fluid injected was CO_2.

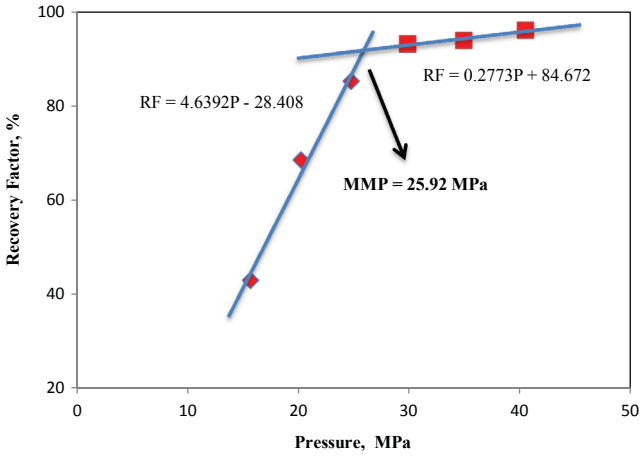

Figure 4

Oil RF *versus* displacement pressure in slim-tube experiment.

3 RESULTS AND DISCUSSION

3.1 Determination of MMP

The MMP is considered as one of the most important parameters in the design of miscible CO_2-EOR projects and criterion of miscibility. To determine the MMP value in this study, six slim-tube experiments were conducted at six different displacement pressures of P between 15.71 and 40.53 MPa and the constant reservoir temperature of 96.1 °C. These pressures were chosen carefully to cover the whole range of an immiscible state to a miscible state. In each pressure, the oil RF after injecting 1.2 PV of CO_2 was recorded and plotted *versus* displacement pressure (Fig. 4). As can be seen, at the pressures less than the MMP, the oil recovery increment is considerable by increasing the pressure but at the pressures higher than the MMP, this oil recovery increment is not significant. Based on the measured data in Figure 4, the oil RF was correlated to the displacement pressure by applying the two linear regressions:

$$\mathrm{RF} = 4.6392P - 28.408 \quad \text{(immiscible region)}. \qquad (4)$$

$$\mathrm{RF} = 0.2773P + 84.672 \quad \text{(miscible region)}. \qquad (5)$$

By equalization the above two equations, the pressure was calculated at the point of intersection of the two linear regressions (break-over point) which this pressure is the same MMP. Therefore, the MMP between CO_2 and the Sarvak heavy oil was determined to be 25.92 MPa at T_{res} = 96.1 °C by using the slim-tube apparatus.

4 COMPARISON OF DIFFERENT FLOODING METHODS

In this research, three different flooding methods of water flooding, miscible continuous CO_2 flooding, and miscible CO_2-WAG flooding were applied to investigate the effect of each of them on the oil RF in the Sarvak formation and select the optimum method with respect to ultimate oil recovery. These experiments involve flooding CO_2 and the synthetic brine continuously and alternately into the oil saturated core samples to reach the ultimate oil RF. In the miscible CO_2-WAG flooding, a total of seven WAG cycles were done with the slug size of 0.15 PV and the WAG ratio of 1:1.

The measured oil RF and oil productions of the water flooding (experiment 1) and the miscible continuous CO_2 flooding (experiment 2) have been shown in Figure 5. As can be seen from this figure, the miscible continuous CO_2 flooding has a higher oil production rate and oil RF than the water flooding, which it is due to a zero CO_2-oil IFT, reduction of oil viscosity and oil swelling. According to Figure 5, water BT occurred at 0.56 PV (the oil RF was 33.1%) in experiment 1. Before water BT, the oil recovery was increased quickly. Nevertheless, only a very small amount of the residual oil (4.6%) was recovered after water BT. This is because the water saturation was increased quickly after water BT and the water channels were established between the inlet and the outlet of the core holder. In contrast to water flooding, the miscible continuous CO_2 flooding in experiment 2 had a different oil production trend after CO_2 BT. As shown in Figure 5, CO_2 BT happened at 0.21 PV (the oil RF was 25.3%). After CO_2 BT, a significant amount of the residual oil (36.2%) was produced. In the miscible continuous CO_2 flooding from 0.95 to 1.25 PV, the oil RF did not increase at all. This is because in the miscible continuous CO_2 flooding from 0.95 to 1.25 PV, a very large amount of CO_2 moved ahead of oil which caused some oil trapping. This factor led to a jump in oil RF of the miscible continuous CO_2 flooding after 1.25 PV.

The measured oil RF and oil productions of the miscible CO_2-WAG flooding (experiment 3) are plotted in Figure 6. As seen in this figure, CO_2 BT occurred at 0.31 PV in the

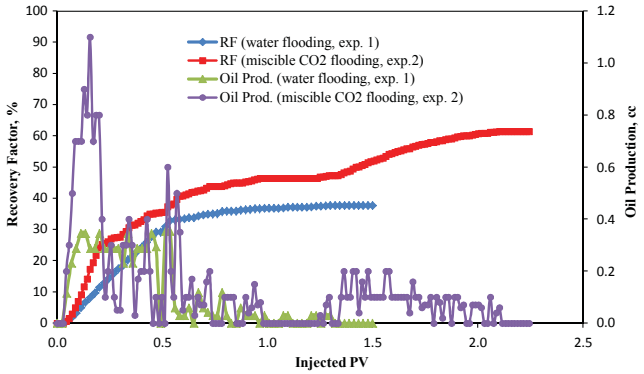

Figure 5

Comparison of oil RF and oil production for water flooding and miscible continuous CO_2 flooding.

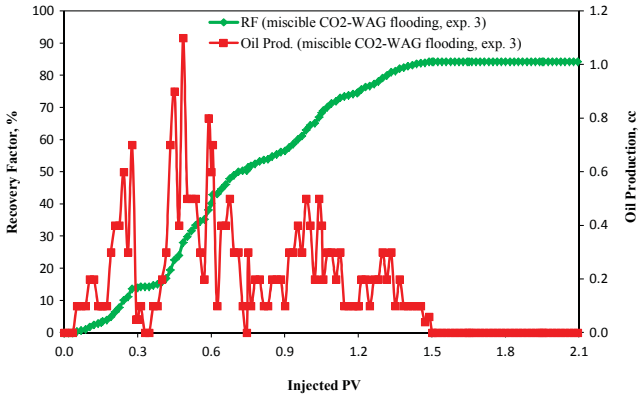

Figure 6

Oil RF and oil production of miscible CO_2-WAG flooding.

second WAG cycle, which was delayed compared to 0.21 PV in the miscible continuous CO_2 flooding. A very large amount of the residual oil (69.9%) was produced after CO_2 BT (25.9%, 16.3%, 18.3%, and 9.4% of the residual oil were recovered in the second, third, fourth, and fifth WAG cycles, respectively, but no more oil was recovered in the sixth and seventh WAG cycles). According to Figure 6, water BT happened at 0.73 PV in the third WAG cycle, which was delayed in comparison with 0.56 PV in the water flooding. The oil RF and oil production rate before water BT is higher than after water BT. This is because the water saturation was gradually increased after water BT and the water channels were gradually formed as far as the water production was increased quickly in the last two WAG cycles. As a result, no more oil was recovered in the last two WAG cycles. As can be seen from Figure 6, the oil RF did not increase at all in a short distance from 0.31 to 0.36 PV. This is because CO_2 BT occurred at 0.31 PV.

The measured oil RF of three different flooding methods are shown in Figure 7. The ultimate oil RF of the miscible CO_2-WAG flooding was the highest (84.3%) at a total of

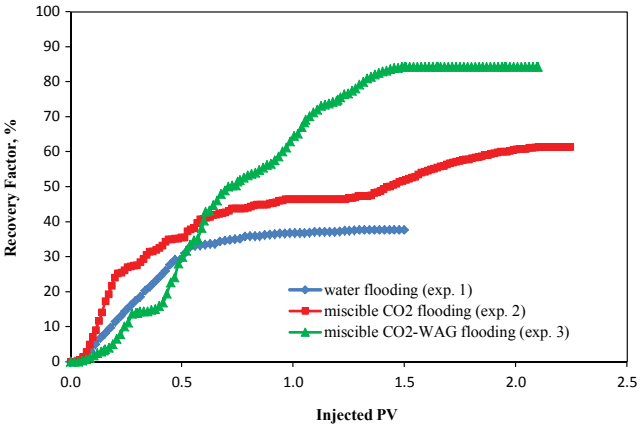

Figure 7

Comparison of oil RF for water flooding, miscible continuous CO_2 flooding, and miscible CO_2-WAG flooding.

2.1 PV of injected CO_2 and brine in comparison with the miscible continuous CO_2 flooding (61.5%) at a total of 2.25 PV of injected CO_2 and the water flooding (37.7%) at a total of 1.5 PV of injected brine. In the miscible continuous CO_2 flooding, a lower viscosity of the injected CO_2 than the residual oil causes increasing the mobility ratio and the resulting viscous fingering and channeling. Also, the gravity overriding occurs due to a high density difference of the injected CO_2 and the residual oil. These results lead to a low volumetric sweep efficiency. In the miscible CO_2-WAG flooding, the injected water controls the mobility and stability of CO_2 displacement front, which causes delaying the gravity overriding and viscous fingering and the resulting a high volumetric sweep efficiency. At the same time, the injected CO_2 under the miscible conditions improves the microscopic displacement efficiency far better than the injected water. Therefore, the miscible CO_2-WAG flooding has a lower residual oil trapped in the Sarvak formation and increases the ultimate oil RF compared to the miscible continuous CO_2 flooding and water flooding.

4.1 The Effect of Slug Size in the Miscible CO_2-WAG Flooding

In this study, to investigate the effect of slug size on the oil RF of the miscible CO_2-WAG flooding, three experiments were performed with different slug sizes of 0.15, 0.25, and 0.50 PV at the WAG ratio of 1:1 (experiments 3–5). In experiments 4 and 5, a total of 2.0 PV of CO_2 and the synthetic brine were injected into the core samples in four and two cycles, respectively. In general, the slug size refers to the volume of the first fluid (CO_2) injected in each cycle and is expressed as a percentage of PV.

The measured oil RF of the three miscible CO_2-WAG flooding experiments are plotted and compared in Figure 8. As shown in this figure, a large amount of the residual oil

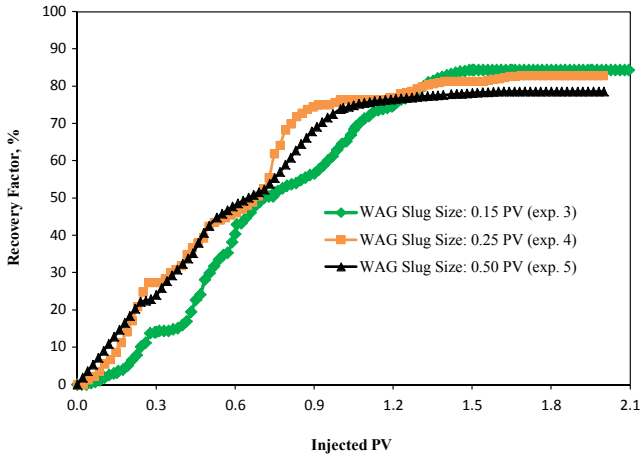

Figure 8

Comparison of oil RF for WAG slug sizes of 0.15, 0.25, and 0.50 PV.

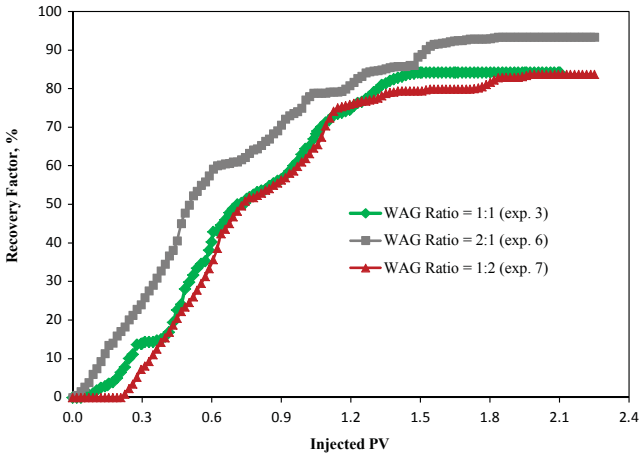

Figure 9

Comparison of oil RF for WAG ratios of 1:1, 2:1, and 1:2.

was recovered in these three experiments before water BT. But after water BT, the oil recovery is lower (water BT of experiments 3–5 occurred at 0.73, 0.75, and 0.83 PV, respectively). The increase of injected water volume in porous media during the miscible CO_2-WAG flooding can cause a waterblocking phenomenon and prevent the injected CO_2 from being contacted with a large amount of the residual oil. This phenomenon, which was found in the water-wet oil reservoir (Huang and Holm, 1988), leads to a severe reduction of the oil RF and oil production rate. Therefore, the miscible CO_2-WAG flooding should be designed so that it does not prevent the injected CO_2 from being contacted with a large amount of the residual oil and does not occur the waterblocking effect.

Figure 8 also shows that the ultimate oil RF of experiment 3 with the slug size of 0.15 PV is the highest (84.3%) in comparison with experiments 4 (82.9%) and 5 (78.6%). This is because experiment 3 has the lowest slug size and its waterblocking effect occurred later than experiments 4 and 5, which the resulting more CO_2 contacted with the residual oil. Hence, the slug size has strong effect on the oil RF of miscible CO_2-WAG flooding. When a large amount of CO_2 contacts with oil under the miscible conditions, a strong mass transfer occurs between CO_2 and oil. As a result, more CO_2 is dissolved inside the oil, which causes a further reduction of oil viscosity and its swell.

Therefore, from the comparison of three miscible CO_2-WAG flooding experiments with the slug sizes of 0.15, 0.25, and 0.50 PV, it can be concluded that experiment 3 with the slug size of 0.15 PV is the most efficient with respect to the ultimate oil RF. Nevertheless, using a smaller slug size increases the operating cost due to a more frequently switch of the fluid injection. Hence, an optimum slug size should be determined for field applications of miscible CO_2-WAG flooding.

4.2 The Effect of WAG Ratio in the Miscible CO_2-WAG Flooding

In this work, to study the effect of WAG ratio on the oil RF of the miscible CO_2-WAG flooding, three experiments were carried out with different WAG ratios of 1:1, 2:1, and 1:2 at the slug size of 0.15 PV (experiments 3, 6, and 7). In experiments 6 and 7, a total of 2.25 PV of CO_2 and the synthetic brine were injected into the core samples in five cycles. In general, the WAG ratio is defined as the ratio of the injected brine volume to CO_2 volume in each cycle.

Figure 9 shows the measured oil RF of three experiments 3, 6, and 7. As can be seen, generally, experiment 6 has a higher oil production rate (the slope of the oil RF *versus* PV injected curve) during the experiment in comparison with experiments 3 and 7. Also, this figure shows that the ultimate oil RF of experiment 6 is the highest (93.4%), which was followed by experiment 3 (84.3%) and experiment 7 (83.7%). Under the miscible conditions, CO_2 has a much higher microscopic displacement efficiency compared to water. At a high WAG ratio, the injected water controls the CO_2 mobility pretty well and a large amount of CO_2 contact with the residual oil, which will lead to a high microscopic displacement efficiency and a great reduction of oil viscosity. On the other hand, the macroscopic displacement (volumetric sweep) efficiency of water is much better than CO_2. Therefore, the oil RF and oil production rate of miscible CO_2-WAG flooding are increased by improving the microscopic and macroscopic displacement efficiencies.

It can be concluded that among the three miscible CO_2-WAG flooding experiments with the WAG ratios of 1:1, 2:1, and 1:2 (experiments 3, 6, and 7), experiment 6 has the best overall performance with respect to its high oil RF, high oil production rate, and low consumption of CO_2. Hence, the miscible CO_2-WAG flooding with the WAG ratio of 2:1 is suitable in this study.

TABLE 4
Oil RF of different cycles in each miscible CO_2-WAG flooding experiment.

Experiment No.	1st cycle		2nd cycle		3rd cycle		4th cycle		5th cycle		6th cycle		7th cycle	
	(%)	(%)	(%)	(%)	(%)	(%)	(%)	(%)	(%)	(%)	(%)	(%)	(%)	(%)
3	3.2	10.8	8.7	17.6	11.2	5.1	11.8	6.5	6.5	2.9	0.0	0.0	0.0	0.0
4	24.8	17.7	19.4	14.5	1.9	3.1	1.5	0.0						
5	42.5	31.4	4.3	0.4										
6	13.5	31.6	15.0	12.9	5.9	6.9	5.7	1.9	0.0	0.0				
7	8.2	14.0	29.6	6.3	18.7	2.7	0.4	3.1	0.7	0.0				

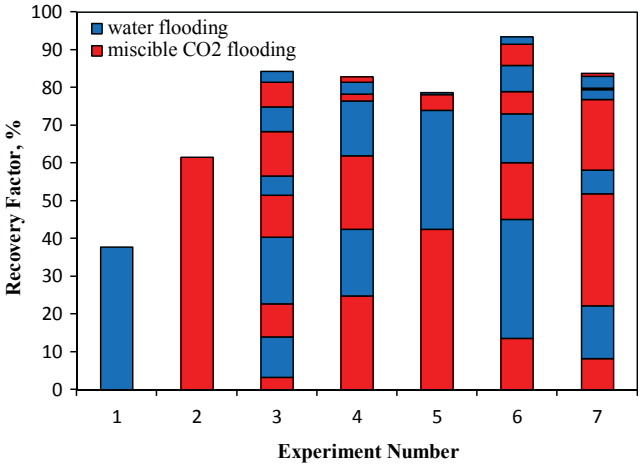

Figure 10
Comparison of oil RF of seven core flooding experiments.

4.3 Oil RF and CO_2 Consumption

The oil RF in each WAG cycle of five miscible CO_2-WAG flooding experiments (experiments 3–7) are summarized in Table 4. Also, the oil RF of all seven core flooding experiments are plotted and compared in Figure 10. Considering Table 4 and Figure 10, the oil RF of the first two cycles of experiments 3–7 are 40.3%, 76.4%, 78.6%, 73.0%, and 58.1%, respectively. A large amount of the heavy oil is produced in the first two cycles in the miscible CO_2-WAG flooding experiments except in experiment 3. The oil RF of the first two WAG cycles and its percentage in the total oil RF of experiment 3 were the lowest because its WAG slug size was 0.15 PV. After the first two WAG cycles in this experiment, a large amount of the residual oil (44.0%) was recovered in the next three WAG cycles. However, experiment 6 with the slug size of 0.15 PV at the WAG ratio of 2:1 had the highest ultimate oil RF and was the most efficient CO_2-WAG flooding method. In this experiment, the injected water can effectively control the mobility of CO_2.

Miscible continuous CO_2 and CO_2-WAG floodings resulted in an unequal amount of cumulative CO_2 injections for each flood. In order to normalize the recoveries, the Tertiary Recovery Factor (TRF) for each experiment was determined. In the literature, the TRF is defined as the percentage of the Residual Oil in Place (%ROIP) divided by the cumulative PV of CO_2 injected (Kulkarni and Rao, 2005). The measured TRF of the miscible continuous CO_2 flooding (experiment 2) and the miscible CO_2-WAG flooding (experiment 6, the most efficient CO_2-WAG flooding method) are shown in Figure 11. As seen in this figure, the miscible CO_2-WAG flooding significantly reduces the CO_2 consumption and enhances the oil RF compared to the miscible continuous CO_2 flooding. On the other hand, gross CO_2 utilization factor for each experiment can be determined. In the literature, the gross CO_2 utilization factor is defined as the volume of CO_2 injected under standard conditions to produce a barrel of oil (Mscf/STB) (Merchant, 2010). The injected CO_2 volumes in experiments 1–7 were equal to 0.00, 2.25, 1.05, 1.00, 1.00, 0.75, and 1.50 PV and the corresponding ultimate oil RF were equal to 37.7%, 61.5%, 84.3%, 82.9%, 78.6%, 93.4%, and 83.7%, respectively. According to the above experimental data, the gross CO_2 utilization factors in experiments 1–7 were approximated to be 0.0, 25.5, 8.7, 8.2, 9.9, 5.8, and 13.0 Mscf/STB. As mentioned in Section 4.3, from the comparison of two miscible CO_2-WAG flooding experiments with the slug sizes of 0.15 and 0.25 PV, the optimal method was selected based on the ultimate oil RF. According to proximity of the oil RF in two experiments and the high CO_2 utilization factor of experiment 3 compared to experiment 4, it is better to be considered the economic conditions in comparing the two experiments. In general, experiment 6 with the slug size of 0.15 PV at the WAG ratio of 2:1 had the highest ultimate oil RF (93.4%), the lowest amount of CO_2 consumption (0.75 PV), and the least CO_2 utilization factor (5.8 Mscf/STB). Therefore, the operating parameters of a CO_2-WAG flooding process, such as its slug size and WAG ratio must be optimized before it is used in a desired oil reservoir.

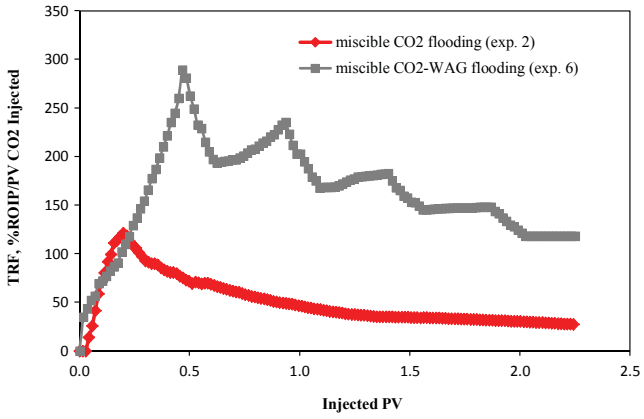

Figure 11

Comparison of TRF for miscible continuous CO_2 flooding and miscible CO_2-WAG flooding.

CONCLUSION

In this research, several slim-tube experiments were done to determine the MMP between the dead oil sample of Sarvak formation and CO_2 at different displacement pressures and the constant reservoir temperature of 96.1 °C. The MMP of 25.92 MPa was determined by plotting the oil RF after 1.2 PV of CO_2 injected *versus* displacement pressure. A total of seven core flooding experiments were performed by using the core samples of Sarvak formation to investigate the performance of the miscible CO_2-WAG flooding process. First, the different flooding methods were studied and compared, *i.e.*, water flooding, miscible continuous CO_2 flooding, and miscible CO_2-WAG flooding. The results showed that the miscible CO_2-EOR process is capable of mobilizing the heavy oil and achieving a high and significant oil RF in the Sarvak formation. This is because under the miscible conditions, the IFT between CO_2 and oil is zero which leads to a high capillary number and microscopic displacement efficiency. The miscible CO_2-WAG flooding has a higher oil RF than the miscible continuous CO_2 flooding and the water flooding by better controlling the mobility of CO_2 and delaying the CO_2 BT. Next, different WAG slug sizes and WAG ratios of the miscible CO_2-WAG flooding were examined and compared. The results also showed that a smaller WAG slug size of 0.15 PV is preferred in the miscible CO_2-WAG flooding. The optimum WAG ratio of the miscible CO_2-WAG flooding for the Sarvak formation is approximately 2:1. In addition, more than 50% of the heavy oil is produced in the first two WAG cycles. The miscible CO_2-WAG flooding has a higher oil production and a less CO_2 consumption than the miscible continuous CO_2 flooding. This means that a CO_2 utilization factor of the miscible CO_2-WAG flooding is lower than the miscible continuous CO_2 flooding. Hence, the miscible CO_2-WAG flooding is considered to be the best CO_2-EOR flooding process in this formation.

ABBREVIATIONS

CO_2-WAG	Water-Alternating-CO_2
EOR	Enhanced Oil Recovery
MMP	Minimum Miscibility Pressure
IFT	Interfacial Tension
BT	Breakthrough
OOIP	Original Oil in Place
RF	Recovery Factor
PV	Pore Volume
BV	Bulk Volume
API	American Petroleum Institute
TDS	Total Dissolved Solids
BPR	Back-Pressure Regulator
HPLC	High Performance Liquid Chromatography
TRF	Tertiary Recovery Factor
ROIP	Residual Oil in Place

REFERENCES

Agbalaka C., Dandekar A.Y., Patil S.L., Khataniar S. (2008) The effect of wettability alteration on oil recovery, in: *SPE 114496, Presented at the SPE Asia Pacific Oil & Gas Conference and Exhibition, Perth, Australia*.

Ahmadi K., (2011) Advances in calculation of minimum miscibility pressure, *Doctoral Dissertation*, University of Texas at Austin.

Alquriaishi A.A., Shokir E.E.M. (2011) Experimental investigation of miscible CO_2 flooding, *Petrol. Sci. Technol.* **29**, 19, 2005-2016.

Baviere M., (1991) Basic concepts in enhanced oil recovery processes, Elsevier Applied Science, Essex, England, UK, p. 221.

Bednarz P., Stopa J. (2014) Enhanced oil recovery methods on offshore fields in the light of world literature, *AGH University of Sci. Technol., Faculty of Drilling, Oil & Gas, Krakow, Poland* **31**, 2, 215-229.

Blunt M., Fayers F.J., Orr F.M. (1993) Carbon dioxide in enhanced: Oil recovery, *Energy Convers. Manage.* **34**, 9, 1197-1204.

Burke N.E., Hoobbs R.E., Kashon S.F. (1990) Measurement and modeling of asphaltene precipitation, *J. Petrol. Technol.* **42**, 1440-1446.

Cao M., Gu Y. (2013) Physicochemical characterization of produced oils and gases in immiscible and miscible CO_2 flooding processes, *Energy & Fuels* **27**, 1, 440-453.

Chen S., Li H., Yang D., Tontiwachwuthikul P. (2010) Optimal parametric design for water-alternating-gas (WAG) process in a CO_2-miscible flooding reservoir, *J. Canadian Petrol. Technol.* **49**, 10, 75-82.

Christensen J.R., Stenby E.H., Skauge A. (1998) Review of WAG field experience, in: *SPE39883, International Petrolium Conference and Exhibition of Mexico*.

Christensen J.R., Stenby E.H., Skauge A. (2001) Review of WAG field experience, *SPE Reservoir Evaluation and Eng.* **4**, 2, 97-106.

Chukwudeme E.A., Hamouda A.A. (2009) Enhanced oil recovery (EOR) by miscible CO_2 and water flooding of asphaltenic and non-asphaltenic oils, *Energies* **2**, 714-737.

Dehghan A., Farzaneh S., Kharrat R., Ghazanfari M., Rashtchian D. (2009) Pore-Level investigation of heavy oil recovery during water alternating solvent injection process, *Transport in Porous Media* **83**, 3, 653-666.

Enick R., Olsen D. (2012) Mobility and conformance control for carbon dioxide enhanced oil recovery (CO_2-EOR) via thickeners, foams, and gels-A detailed literature review of 40 years of research, contract DE-FE0004003, Activity 4003.200.01, National energy technology laboratory (NETL), Pittsburgh.

Farouq A. (2003) The unfulfilled promise of enhanced oil recovery-More Lies Ahead. *SPE London Section Presentation*.

Farshid T., Benyamin Y.J., Ostap Z., Brett A.P., Nevin J.R., Ryan R. W. (2010) Effect of oil viscosity, Permeability and injection rate on performance of waterflooding, CO_2 flooding and WAG processes on recovery of heavy oils, in: *SPE 138188, Canadian Unconventional Resources and International Petroleum Conference, Calgary, Alberta, Canada*.

Gale J.J., (2003) Opportunities for early applications of CO_2 sequestration technology, *IEA Greenhouse Gas R&D Program File Note*.

Ghedan S. (2009) Global laboratory experience of CO_2-EOR flooding, in: *SPE 125581, SPE/EAGE Reservoir Characterization and Simulation Conference, Abu Dhabi, UAE*.

Grigg R.B., Schecter D.S. (1993) State of the industry in CO_2 floods, in: *SPE 38849, Presented at the SPE Annual Technical Conference and Exhibition, Texas, San Antonio*.

Hamouda A.A., Chukwudeme E.A., Mirza D. (2009) Investigating the effect of CO_2 flooding on asphaltenic oil recovery and reservoir wettability, *Energy & Fuels* **23**, 1118-1127.

Holt T., Lindeberg E., Wessel-Berg D. (2009) EOR and CO_2 Disposal-economic and capacity potential in the north sea, *Energy Procedia* **1**, 1, 4159-4166.

Huang E.T.S., Holm L.W. (1988) Effect of WAG injection and rock wettability on oil recovery during CO_2 flooding, *SPE Reservoir Eng.* **3**, 1, 119-129.

Idem R.O., Ibrahim H.H.J. (2002) Kinetics of CO_2-induced asphaltene precipitation from various saskatchewan crude oils, *J. Petrol. Sci. Eng.* **35**, 233-246.

Kulkarni M.M., Rao D.N. (2005) Experimental investigation of miscible and immiscible water-alternating-gas (WAG) process performance, *J. Petrol. Sci. Eng.* **48**, 1, 1-20.

Majidaie S., Khanifar A., Tan I.M., Onur M. (2013) The potential of immiscible carbon dioxide flooding on malaysian light oil reservoir, *Int. J. Petrol. Geosci. Eng.* **1**, 1, 1-11.

Manrique E., Thomas C., Ravikiran R., Izadi M., Lantz M., Romero J., Alvarado V. (2010) EOR: Current status and opportunities, in: *SPE-130113, Presented at the SPE Improved Oil Recovery Symposium, Tulsa, Oklahoma*.

Merchant D.H. (2010) Life Beyond 80: A look at conventional WAG recovery beyond 80% HCPV injected in CO_2 tertiary floods, in: *SPE 139516, Presented at the SPE International Conference on CO_2 Capture Storage and Utilization, New Orleans, Louisiana*.

Mirkalaei S.M., Hosseini S., Masoudi R., Demiral B.M., Karkooti H. (2011) Investigation of different I-WAG schemes toward optimization of displacement efficiency, in: *SPE EOR Conference, Kuala Lumpur, Malaysia*, pp. 1–12.

Moritis G. (2006) EOR survey, *Oil & Gas J.* **15**, 37-57.

Rao D.N., Girard M. (2002) Induced multiphase flow behaviour effects in gas injection EOR projects, *J. Canadian Petrol. Technol.* **41**, 7, 53-60.

Righi E.F., Pascual M. (2007) Water-alternating-gas pilot in the largest oil field in argentina: Chihuido de la Sierra Negra, Neuquen Basin, in: *Latin America and Caribbean Petroleum Engineering Conference, Buenos Aires*, pp. 1–9.

Rogers J.D., Grigg R.B. (2000) A literature analysis of the WAG injectivity abnormalities in the CO_2 process, in: *SPE 59329, Presented at the SPE Improved Oil Recovery Symposium, Tulsa, Oklahoma*.

Rouzbeh G.M., Larry W.L. (2010) Simultaneous water-gas-injection performance under loss of miscibility, in: *SPE 129966, Presented at the SPE Improved Oil Recovery Symposium, Tulsa, Oklahoma*.

Skauge A., Stensen J.A. (2003) Review of WAG field experience, in: *International Conference and Exhibition, Modern Challenges in Oil Recovery, Gubkin University, Moscow, Russia*.

Sohrabi M., Tehrani D.H., Danesh A., Henderson G.D. (2004) Visualization of oil recovery by water-alternating-gas injection using high-pressure micromodels, *SPE J.* **9**, 3, 290-301.

Sohrabi M., Emadi A., Jamiolahmady M., Ireland S., Brown C. (2008) Mechanisms of extra-heavy oil recovery by gravity oil recovery stable CO_2 injection, in: *SCA 2008-20, Presented at the International Symposium of the Society of Core Analysis, Abu Dhabi, UAE*.

Song Z., Li Z., Wei M., Lai F., Bai B. (2014) Sensitivity analysis of water-alternating-CO_2 flooding for enhanced oil recovery in high water cut oil reservoirs, *Computers & Fluids* **99**, 93-103.

Tunio S.Q., Tunio A.H., Ghirano N.A., El Adawy Z.M. (2011) Comparison of different enhanced oil recovery techniques for better oil productivity, *Int. J. Appl. Sci. Technol.* **5**, 1, 143-153.

Manuscript submitted in 9 June 2016
Manuscript accepted in 11 September 2017
Published online in November 2017